Fracture Mechanics of Concrete Structures
Proceedings FRAMCOS-3
AEDIFICATIO Publishers, D-79104 Freiburg, Germany

FRACTURE MECHANICS STUDY OF CONCRETE BEAMS REINFORCED WITH FRP SHEETS BY A MOMENT TENSOR ANALYSIS OF ACOUSTIC EMISSION

Z. W. Li and S. Yuyama
Nippon Physical Acoustics LTD., Tokyo, Japan

I. Ohsawa, I. Kimpara, K. Kageyama and K.Yamaguchi
Department of Naval Architecture and Ocean Engineering, Graduate School of engineering, The University of Tokyo, Japan

Abstract

Center notched concrete beams reinforced with carbon and glass fiber reinforced plastic sheets were subjected to three-point flexure loading. Conventional AE parameter analysis showed that the beginning of continuous occurrence and exponentially increment of AE activities corresponds to the critical load at which the crack initiates at the notch tip. The critical stress intensity factor of the notch tip was calculated based on the crack tension method using the estimated critical load. A moment tensor analysis was applied to the AE waveform sets recorded at six sensors. On the basis of the arrival time differences and the amplitudes of the first motions of the AE waveforms, crack locations were determined and AE source was classified into a tensile crack or a shear crack. The failure process resulted form the moment tensor analysis was in good agreement with visual observations.
Key words: Acoustic emission, moment tensor analysis, infrastructure, FRP sheets, concrete beams, fracture mechanics

1 Introduction

Recently rehabilitation of infrastructure damaged by earthquake, fatigue, overload or severe and long term environmental attacks during service has become a great problem. Bonding thin steel plates to critical areas of concrete subjected to tensile loading has been shown to be an effective strengthening method. Over the past decade, high strength, light weight fiber reinforced plastics (FRP), primarily developed for aerospace and other industrial applications, have been successfully used in concrete structural members (Kageyama et al., 1995; Shahawy et al., 1996).

The bonding of thin FRP laminates exhibits an effective strengthening in tension in the critical tensile zone of concrete structures. The advantage of this system is the simplicity of application relative to the bonding of steel plates. Thus in order to reinforce the existing concrete structures, carbon and glass fiber reinforced plastic (CFRP, GFRP) sheets are widely applied in such structures as pillars, beams, slabs and so on. In the meantime, research on the experimental characterization of reinforcing effects of these FRP sheets reinforced concrete structures has become an urgent need. Since acoustic emission (AE) is very sensitive to the initiation and propagation of cracks in concrete, it is a very useful technique to monitor failure process of concrete structures.

There are two ways to analyze AE data acquired by conventional AE instrument. The first one is parameter analysis, which has been widely and more frequently employed. It analyzes relative AE activities based on the measurement of parameters such as hit, count, energy, amplitude and so on. The second, which has made a remarkable progress for the last ten years, is quantitative waveform analysis such as the moment tensor analysis using the SiGMA (simplified Green's function for moment tensor analysis) code (Ohtu, 1995; Yuyama et al., 1995). Quantitative information on AE sources is analyzed by applying theoretical treatment to the waveforms recorded from more than six sensors. First using the arrival time differences, three dimensional crack location is calculated. Then moment tensor components are determined from the amplitudes of the first motions of AE waveforms. On the basis of the eigenvalue analysis of the moment tensor, AE source is classified into a tensile crack and a shear crack. Furthermore, crack orientation is determined from the eigenvectors.

In the present paper, the focus is on the experimental evaluation of reinforcing effects of FRP sheets externally bonded to the bottom tensile zone of concrete beam specimens in terms of failure process and increased fracture toughness, by applying both AE parameter and moment tensor analysis.

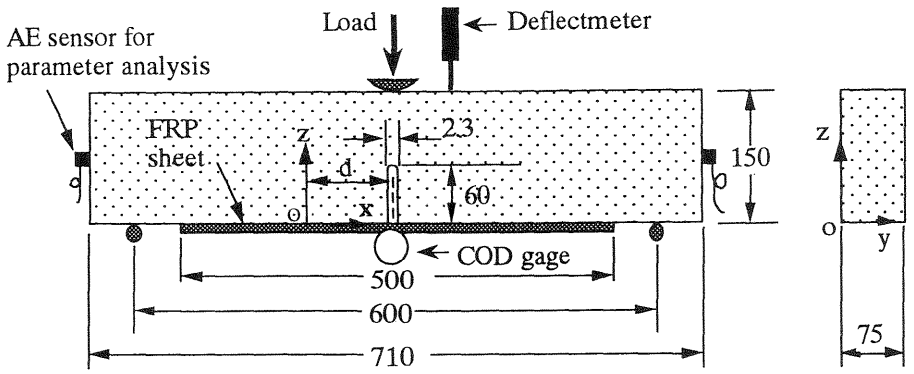

x-y-z: AE sensor coordination for moment tensor analysis
d=100mm for specimen without reinforced FRP sheet
d=10mm for specimen with reinforced FRP sheet

Fig. 1. Details of concrete specimen with a center notch.

Table 1. Mix proportion of the concret

Water Cement Ratio (%)	Sand Percentage (%)	Mix Proportion (kg/m^3)			
		Water	Cement	Fine Aggregate	Coarse Aggregate
55	45	318	176	818	988
Tensile Strength: 3.6 MPa		Compressive Strength: 26.6 MPa			

2 Experiment

2.1 Concrete specimen and test method

In this study, concrete specimens with a center notch were prepared for the experiment. Shown in Fig. 1 are dimensions of the specimen, which was based on the test method of RILEM (Shah et al.). Mix proportion, compressive strength and tensile strength of the concrete are given in Table 1. For the reinforcement of the specimen, three kinds of condition were considered. One was bonded with one ply of CFRP sheet externally on the bottom tensile zone, another was one ply of GFRP sheet and the other was without reinforcement.

Figure 2 shows the experimental set up for three-point-flexure test with a specimen and a total of eight acoustic emission (AE) sensors.

2.2 AE measurement

A six channel Physical Acoustics MISTRAS 2001 system was utilized to record AE waveforms for the moment tensor analysis. Another two channel MISTRAS system was employed for the measurement of conventional AE

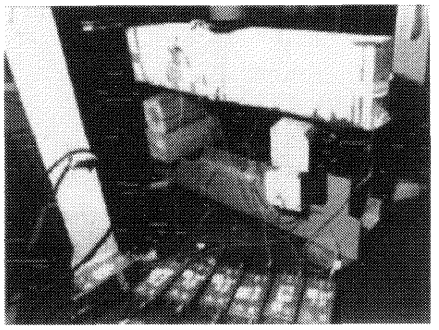

Fig. 2. Experimental setup of three-point-flexure test

Table 2. Location and direction of AE sensors for moment tensor analysis

CH	Specimen with FRP Sheet						Specimen without FRP Sheet					
	Location (m)			Direction (cosine)			Location (m)			Direction (cosine)		
	x	y	z	x	y	z	x	y	z	x	y	z
1	0.180	0.008	0.000	0.0	0.0	1.0	0.000	0.055	0.000	0.0	0.0	1.0
2	0.030	0.075	0.010	0.0	-1.0	0.0	0.200	0.020	0.000	0.0	0.0	1.0
3	0.000	0.000	0.140	0.0	1.0	0.0	0.000	0.020	0.150	0.0	0.0	-1.0
4	0.110	0.038	0.150	0.0	0.0	-1.0	0.200	0.055	0.150	0.0	0.0	-1.0
5	0.160	0.075	0.120	0.0	-1.0	0.0	0.050	0.075	0.130	0.0	-1.0	0.0
6	0.110	0.000	0.030	0.0	1.0	0.0	0.150	0.000	0.130	0.0	1.0	0.0

parameters. AE signals were detected by eight PAC R15 (150kHz resonant type) sensors. Six of them were used for moment tensor analysis and other two were arranged for conventional AE measurement. AE sensor locations and direction cosines of the detecting directions are summarized in Fig. 1 and Table 2.

In the present study, AE signals detected by the sensors were bandpassed by a 100kHz to 300kHz filter and amplified to 40dB in 1220A preamplifiers. For the moment tensor analysis, the threshold of the predetermined trigger channel was set to 50dB. Waveforms were recorded with a sampling speed of 2MHz and a sampling length of 2k words. The wave velocity of the concrete specimen was referred to as 4000m/sec.

3 Results and discussions

3.1 Critical load evaluated by AE and stress intensity factors

To evaluate the critical load, the 5% offset procedure by the RILEM test method and the method for metallic material can be normally used. However, in the case of present study stable values could not be obtained, there-

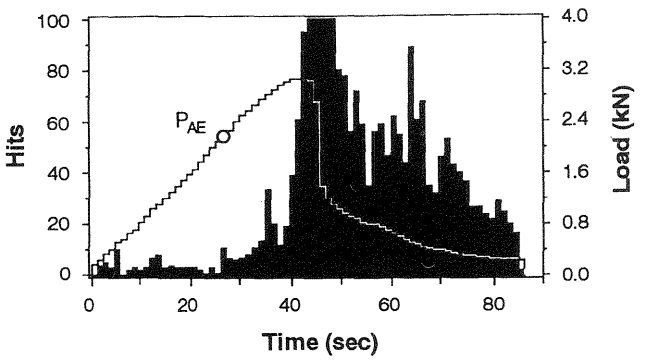

Fig. 3. AE behaviors and load history of concrete specimen

Table 3. Comparison of experimental P_{AE} and stress intensity factor K_{IC} calculated by FEM

	GF:1 ply	CF: 1ply	Concrete
P_{AE}(N)	3860	6220	2350
K_{IC}(MPa $m^{1/2}$)	0.424	0.499	0.595

fore the AE technique was applied. When AE activities became continuous and AE hit rate began to increase exponentially, the corresponding load was defined as "P_{AE}" as shown in Fig. 3. By using finite element analysis based on the condition of two dimensional plane strain and assuming perfect bonding of the interface between concrete and reinforcement layer, the critical stress intensity factor "K_{IC}" of the notch tip was calculated on the basis of the crack extension method by using P_{AE} as shown in Table 3. Most of the K_{IC} values were about 0.5MPa $m^{1/2}$, and the difference in value was small compared to the non-reinforced specimen. Therefore, the results showed that crack initiation does not depend on the reinforcement. That is to say, the crack initiation depends on the fracture toughness of concrete itself. Thus it was verified that the AE technique detects crack initiation effectively.

3.2 Results of moment tensor analysis

Figure 4, Fig. 5 and Fig. 7 show the moment tensor analysis results for center notched concrete specimens. In these figures, tensile cracks (the shear ratio x<40%) are indicated by arrows (⇔), the orientation of which is in accordance with the crack opening direction. Shear cracks (x>60%) are plotted by crosses (×). One of the two orientations of the crosses corresponds to the direction of shear crack motion. Medium cracks (40%<x<60%) are given by the combination of the two symbols.

Loading history showing every failure stage of the specimens obtained

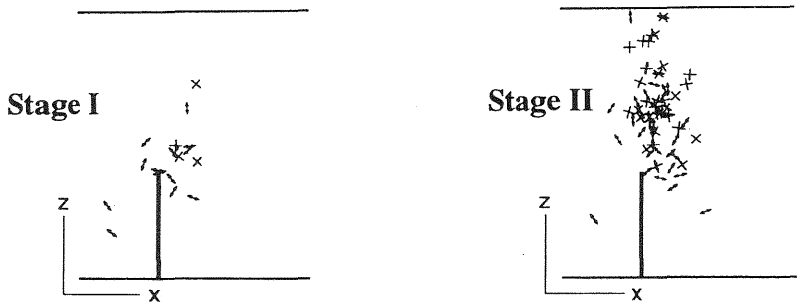

Fig. 4. Moment tensor analysis results for concrete specimen

from moment tensor analysis are demonstrated in Fig. 8.

3.2.1 Results for specimen without FRP sheet reinforcement

As shown in Fig. 4 for a center notched concrete specimen without FRP sheet reinforcement, the failure mode is very simple. Crack initiates and propagates vertically from the tip of the notch. The failure process could be divided into two stages according to the load. The first stage corresponds to loading up to the maximum load (about 3060N, see Fig. 8), in which case cracks only occurred at a area near the notch tip. After the maximum load, cracks grew rapidly upward and the specimen failed. The first stage took about 40 minutes, while the second stage completed only in few minutes.

3.2.2 Results for specimen reinforced with FRP sheet

Moment tensor analysis results showing failure process, crack location, crack type and orientation for center notched concrete specimens reinforced with CFRP and GFRP sheet are demonstrated in Fig. 5 and Fig. 7.

Fig. 6 shows the typical failure mode of a reinforced specimen. Crack ① initiates and propagates vertically from the tip of the notch at first.

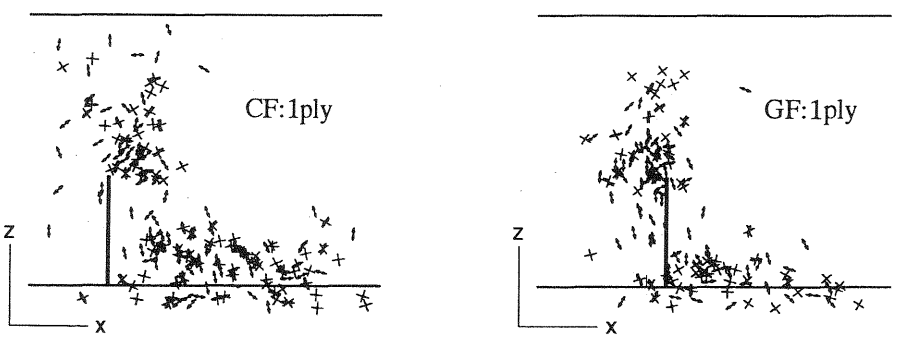

Fig. 5. Moment tensor analysis results for concrete specimens reinforced with CFRP sheet and GFRP sheet

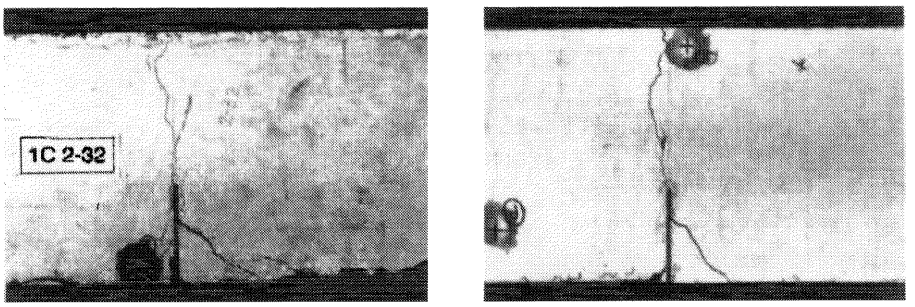

Fig. 6. Photographs of failed specimen with reinforced CFRP sheet (left) and GFRP sheet (right)

Next, 45-degree cracks ② occur from the bottom to the center of the specimen. Finally, crack ③ at the bottom of the specimen extends from initiation point of the 45-degree crack to the direction of support of the flexural jig. The interface of the bottom crack was in the concrete and not between concrete and reinforcement layer, which verified the excellent bonding. Although composition of the concrete is non-homogeneous, the results of the analysis shown in Fig. 5 are apparently in good agreement with the above failure mode.

Regarding the failure progress, as shown in Fig. 7, three different stages can be observed according to process. In the first stage, only main cracks occurred within a area near the notch tip. Since no crack is detected from the bottom of the specimen, the reinforcing effect is operating in this stage. The first stage is corresponding to the load below 6940N (point C①, see Fig. 8) for the case of CFRP sheet reinforcement and 5600N (point G①, see Fig. 8) for the case reinforced by GFRP sheet. In the second stage, the main cracks of the notch tip grew rapidly upward and at the same time cracks also initiated and propagated in the regions of 45-degree direction and the bottom of the specimen. The second stage corresponds to the load between 6940N to 9800N (point C① to point C②, see Fig. 8) for the case of CFRP sheet reinforcement and between 5600N to 8300N (point G① to point G②, see Fig. 8) for the case reinforced by GFRP sheet. In this stage, the effect of the FRP sheet reinforcement became weaker and weaker gradually along with the initiation and growth of the bottom cracks. The third stage corresponds to the load beyond 9800N for the case of CFRP sheet reinforcement and 8300N for the case reinforced by GFRP sheet. From Fig. 7, it is seen that in this stage the main cracking is finished (it could be considered that the main cracks have reached the upper surface of the specimen) and only cracks in the bottom of the specimens continued to propagate towards the support of the flexural jig.

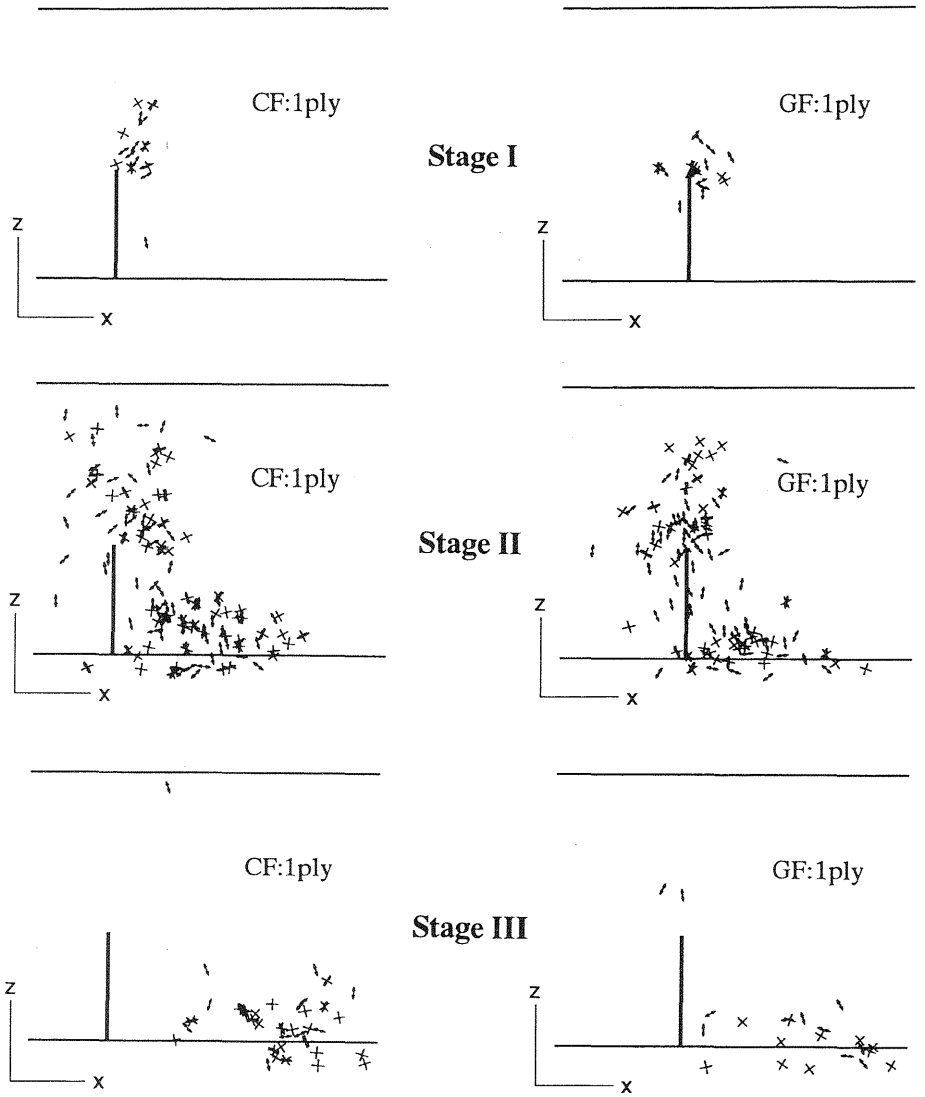

Fig. 7. Moment tensor analysis results showing staged failure process for concrete specimens reinforced with CFRP sheet (left figure) and GFRP sheet (right figure)

Table 4 gives the percentage of shear cracks occurred during each stage of the failure for the three specimens. In the first stage, either the specimen with or without FRP sheet reinforcement has the same value of about 20%. Moreover, in the three stages, both of the specimens reinforced with CFRP and GFRP sheet have similar values of shear crack percentage.

Comparing the failure process of the specimen with reinforced FRP sheet to that without FRP sheet in the loading history shown in Fig.8, the follow-

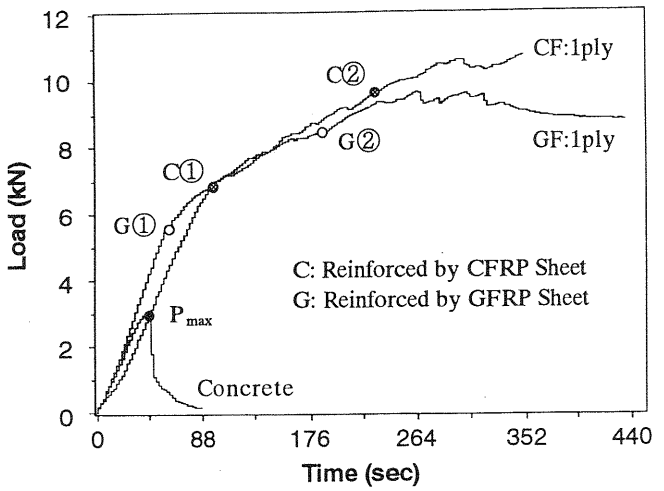

Fig. 8. Loading history showing every failure stage for concrete specimens with and without FRP sheet reinforcement

Table 4. Percentage of shear crack for each of the failure stage

Specimen	Percentage of Shear Crack (%)		
	Stage I	Stage II	Stage III
Concrete	22	39	–
CF: 1 ply	20	26	38
GF: 1 ply	21	28	48

ing results are summaried.

1. The loading curve of the specimen with reinforced FRP sheet did not give a clear maximum value like that of the specimen without reinforced FRP sheet. Till the point C① and G① the FRP reinforced specimens have a similar failure behavior with the specimen without reinforced FRP sheet. The crack type, the crack areas and the number of cracks are similar. Therefore the point C① and G① can be referred to as "equivalent maximum load". The "equivalent maximum load" is about two times of the maximum load of the specimen without reinforced FRP sheet.
2. In the case of specimen without reinforced FRP sheet, after the load reached the maximum load crack growth became unstable and the crack grew so rapidly from the notch tip that the specimen failed at once. For the FRP reinforced specimens, after the "equivalent maximum load" the 45-degree crack and the bottom crack occurred. However, the propagation of the main crack is still stable and relatively slow.

4. Conclusions

The failure process and reinforcing effects of concrete specimens strengthened externally by bonding FRP sheets to the bottom tensile zone were characterized by applying both the AE parameter analysis and moment tensor analysis. From the experimental results the following conclusion can be drawn:

1. It was shown that AE techniques detect crack initiation, source location and can classify crack type and orientation effectively.
2. With the reinforcement of FRP sheet, the critical load (P_{AE}) and the maximum load (equivalent maximum load) of the center notched specimen greatly increased. Moreover, the reinforcing effect of the CFRP sheet was more efficient than that of the GFRP sheet.
3. Regarding the failure process after the equivalent maximum load, the crack growth of a FRP sheet reinforced specimen is still stable and slow for a rather long period.

5. References

Kageyama, K., Kimpara, I. and Esaki, K. (1995) Fracture mechanics study on rehabilitation of damaged infrastructures by using composite wraps, in **10th Intern. Conf. on Composite Materials (ICCM-10)** (eds.A. Poursartip and K. Street), Whistler, B.C., Canada, III-597-604.

Ohtsu, M. (1995) Acoustic emission theory for moment tensor analysis, **Res. Nondestr. Eval.,** 7-6, 169-184.

Shahawy, M. A., Arockiasmy, M., Beitelman, T. and Sowrirajan, R. (1996) Reinforced concrete rectangular beams strengthened with CFRP laminates, **Composite: Part B**, 27B, 225-233.

Shah, S. P. and Carpinteri, A. Fracture mechanics test method for concrete, **RILEM Committee 89-FMT (International Union of Testing and Research Laboratories for Materials and Structures)**, CHAPMAN AND HALL.

Yuyama, S., Carlos, M. F. and Vahavious, S. J. (1995) Development of a moment tensor analysis system for quantitative acoustic emission evaluation, in **8th Asia-Pacific Conf. on NDT (8th APCNDT),** Taipei, Taiwan, 363-372.